# MERIS INSTRUMENT CALIBRATION

**Ludovic Bourg[1], Steven Delwart[2]**

*[1] ACRI-ST, 260 route du Pin Montard, BP 234, 06904 Sophia-Antipolis Cedex, France, Email: lb@acri-st.fr*
*[2] ESA/ESTEC, P.O. Box 299, 2200AG Noordwijk, The Netherlands, Email: Steven.Delwart@esa.int*

## ABSTRACT

The paper intends to describe the operational processing of the MERIS Radiometric Calibration and its present status. An overview of the instrument, the principles of its radiometric calibration and an outline of the calibration processing chain are presented. The various models used within the calibration processing are described and discussed. A status of the error budgets and uncertainties of on-ground and in-flight measurements, of models performances, and finally of the expected radiometric accuracy is given.

## 1 OVERVIEW OF THE INSTRUMENT

MERIS is a programmable, medium-spectral resolution, imaging spectrometer operating in the reflective solar spectral range (390 nm to 1040 nm). Its fifteen spectral bands are programmable by ground command both in width and in position by steps of 1.25nm.

The instrument scans the Earth's surface using the 'push broom' method where the spectral signal is dispersed to illuminate a 2-D detector array for each scan line. The spectral bands are constructed by first binning spectral samples directly on the array into micro-bands, and further grouping them into bands digitally before transmission to ground (See fig.1).

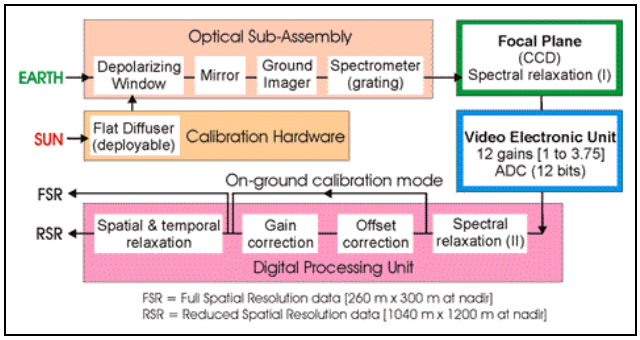


Figure 1: Instrument concept

The instrument has a field of view of 68.5° and covers a swath width of 1150 km. The field of view is shared between five identical optical modules arranged in a fan shape configuration.

The earth is imaged at a spatial resolution of 300 m (at nadir). The reduced resolution data (1200 m) is computed by the on-board combination of four adjacent samples across track over four successive lines. The low rate reduced resolution (RR) data will be acquired systematically, while the high rate full resolution (FR) data will be recorded in parallel according to user requests for a maximum duration of 20 minutes per orbit.

## 2 MERIS RADIOMETRIC CALIBRATION PRINCIPLE

MERIS calibration is based on on-board measurements of Sun light. It is performed at the orbital South Pole where diffuser plates are deployed by rotating a selection disk (See fig.2) into any of the five positions described below:

- Shutter: Is used for dark calibration as well as for protecting the instrument from contaminants,
- Earth observation**:** A diaphragm is introduced in the field of view.
- Radiometric calibration**:** The sun illuminates a white diffuser plate inserted in the field of view
- Diffuser degradation monitoring**:** A second white diffuser plate will be deployed every 3 months to monitor the degradation of the frequently used plate.
- Spectral calibration**:** An Erbium doped "Pink" diffuser will be deployed with MERIS configured to sample its absorption features. Spectral absorption features introduce in the reflectance spectrum by Erbium allows to accurately monitor MERIS spectral behaviour.

The radiometric calibration of MERIS is performed with the use of the two on-board sun-lit radiometric (white) calibration diffuser plates described above. The diffuser plates, made of Spectralon™, provide a uniform illumination signal over the large field of view of the instrument.

MERIS Calibration thus rely on Sun diffusers characterisation and on-board measurements. Its processing uses the same radiometric model of the instrument than Earth Observation processing.
It can be summarised in four main steps:

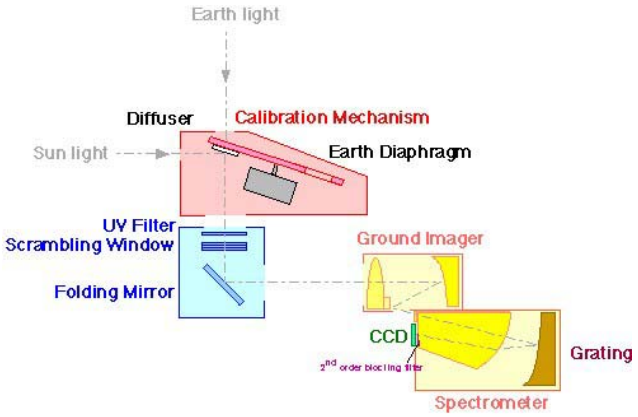


*Figure 2: Optical concept*

1. A radiometric calibration measurement provides instrument numerical counts $X_{cal}(\lambda,k)$, where $\lambda$ stands for the spectral channel and k for the spatial position.
2. Instrumental corrections (non-linearity, dark offset, smear) yields *corrected counts*, $X'_{cal}(\lambda,k)$, considered as perfectly proportional to the radiance at instrument entrance.
3. Instrument Gain Coefficients G are then computed such as

$$X'_{cal}(\lambda,k) = G(\lambda,k).L_{cal}(\lambda,k) \quad (1)$$

4. $L_{cal}$ is estimated from $E_0(\lambda)$, the Sun extraterrestrial Irradiance at the MERIS channel wavelength, illumination and viewing geometry and the diffuser BRDF (bi-directional reflectance distribution function).
   a. The diffuser BRDF has been characterised on-ground
   b. E0 is derived from a model [1], the seasonal variation of the Sun-Earth distance, and the instrument spectral characterisation (channels central wavelengths and spectral response curves).
   c. Geometry is derived from Satellite position and attitude computations and instrument pointing characterisation.

Exposure of the instrument to space environment implies ageing of its components, including diffuser plates and optics. If ageing of the sensor itself is inherently part of the instrument response, and as such must be accounted for in the Gain Coefficients computation, ageing of the diffuser plate impacts the estimation of the radiance at instrument entrance. It is thus necessary to monitor and quantify this ageing independently, thanks to a second diffuser plate, used much less frequently.

There are two possible approaches to handle the variation of the instrument response with time: the first one is to frequently update the calibration coefficients, the second one is to model their evolution with time.

## 3 CALIBRATION PROCESSING CHAIN

The processing chain from instrument acquisitions to calibrated top of atmosphere (TOA) radiances is outlined in Fig. 3.

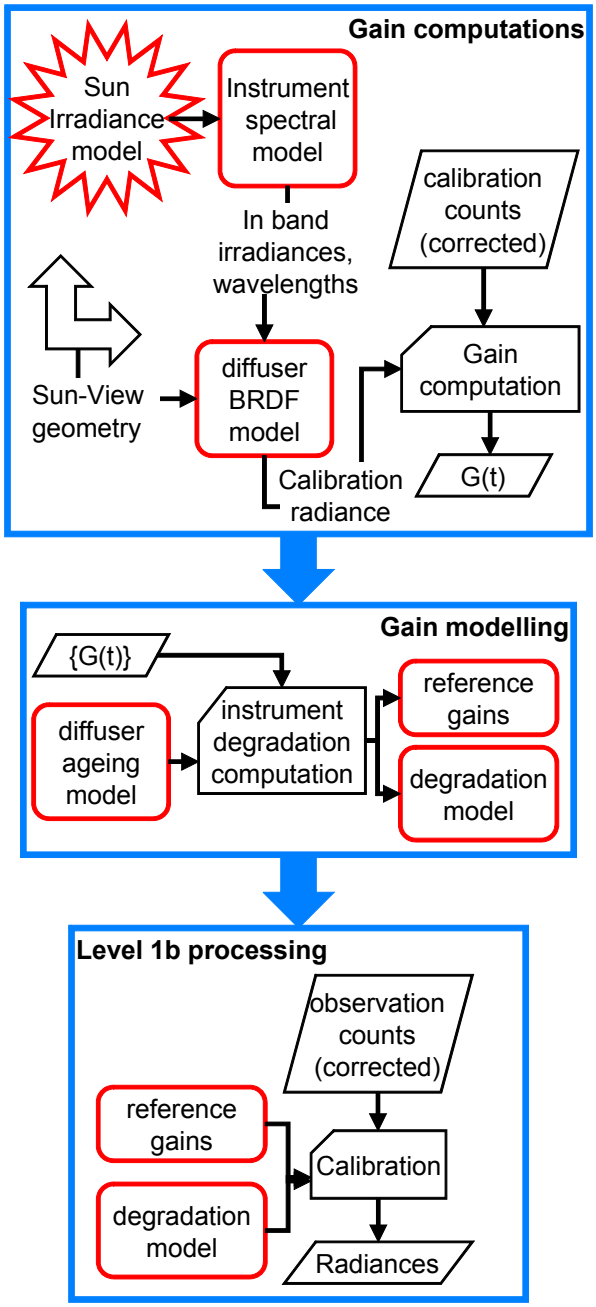


*Figure 3: MERIS Calibration processing chain. Red symbols indicate the use of models.*

It includes:

1. the gain computations, or processing of the on-board radiometric calibration data into instantaneous gain coefficients

2. the gain modelling that, for a given set of instantaneous gain coefficients, allows to model the sensor degradation and derive reference gains – or gain coefficients valid for a reference time – and a model of instrument degradation – i.e. a mathematical representation of the variation with time of the gain coefficients
3. the calibration itself, within the Level 1b processing, of the Earth observation data, that is the conversion of instrument digital counts into top of atmosphere radiance.

## 4 MERIS CALIBRATION DATA

Radiometric calibration measurements, using the nominal diffuser (hereafter referred to as diffuser 1) are performed nominally every two weeks. Measurements dedicated to the monitoring of the diffuser ageing are performed every three months. They consist in measurements with the nominal (diffuser 1) and the reference diffuser (diffuser 2) on two successive orbits, thus minimizing the differences between the two measurements conditions.

At present, four yeas after launch, a total of 94 diffuser 1 calibrations and 17 diffuser 2 calibrations are available. They are regularly spread over time, except for the very first weeks of the mission due to progressive implementation of the operational capacities. This time spread is illustrated on Fig. 4 below for diffuser 1 (blue diamonds) and diffuser 2 measurements (red circles).

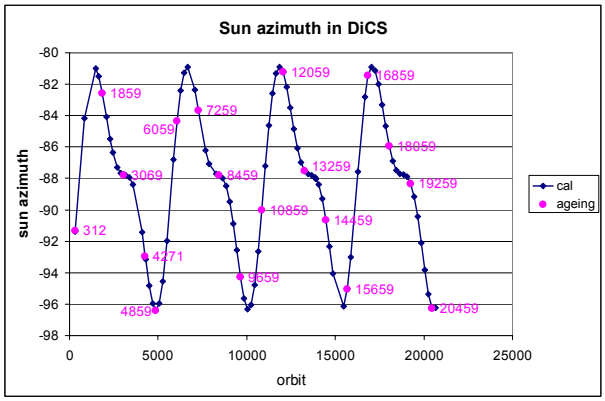


*Figure 4: available radiometric calibration data. Measurements of Diffuser 1 (blue diamonds) and diffuser 2 (red circles) are shown as Sun Azimuth angle vs. orbit number. Orbit scale can be converted into time with the approximate ratio of 5000 orbits per year.*

## 5 MODELS USED IN MERIS CALIBRATION

The following models are used within MERIS calibration processes:

1. Computation of Calibration radiance
   a. Irradiance Model [1]
   b. Instrument spectral model
   c. Diffuser BRDF model for both diffusers (from on-ground characterisation)
   d. Diffuser ageing
2. Instrument degradation model

The irradiance model is not discussed here. It has been selected by the European Space Agency as the standard. Instrument spectral model is not described as it is discussed in a specific communication in the same Conference [2]

### 5.1 Diffuser BRDF model

#### 5.1.1 Diffuser BRDF characterisation

The diffuser plates, made of Spectralon$^{TM}$, provide a uniform illumination signal over the large field of view of the instrument.
The calibration plates have been extensively characterised on-ground using a dedicated BDRF bench (See fig.4 and 5) to an absolute accuracy of better than 1%. This performance estimate was confirmed by a round-robin exercise performed with other laboratories (i.e. NIST, NASA, NPL).

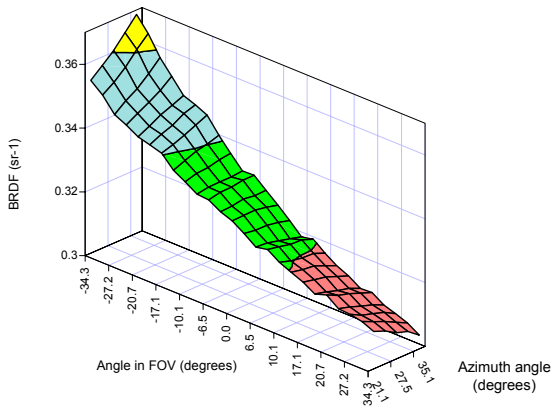


*Figure 4: Diffuser plate 1 BRDF at 410 nm for four illumination conditions corresponding to different times throughout the year.*

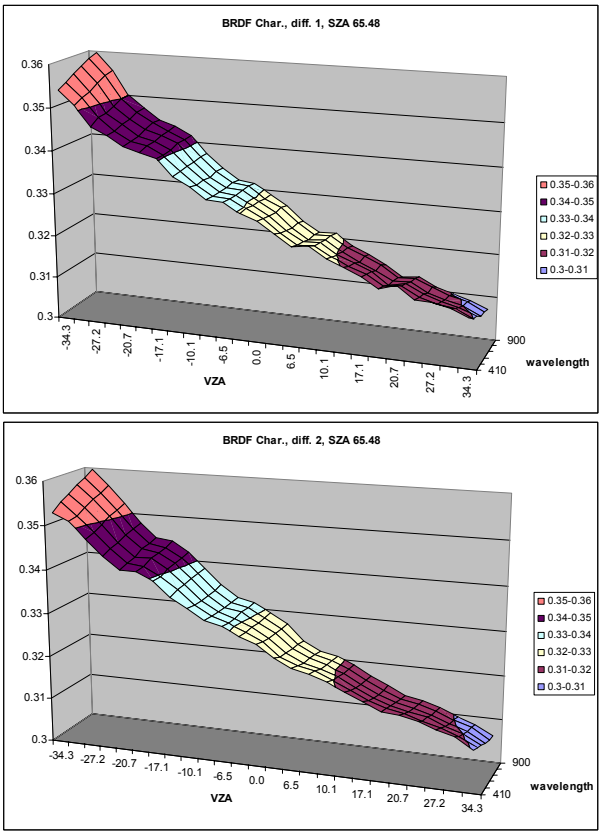


*Figure 5: Diffuser plate 1 (top) and 2 (bottom) BRDF for a given illumination condition as a function of the viewing zenith angle (VZA axis) and wavelength.*

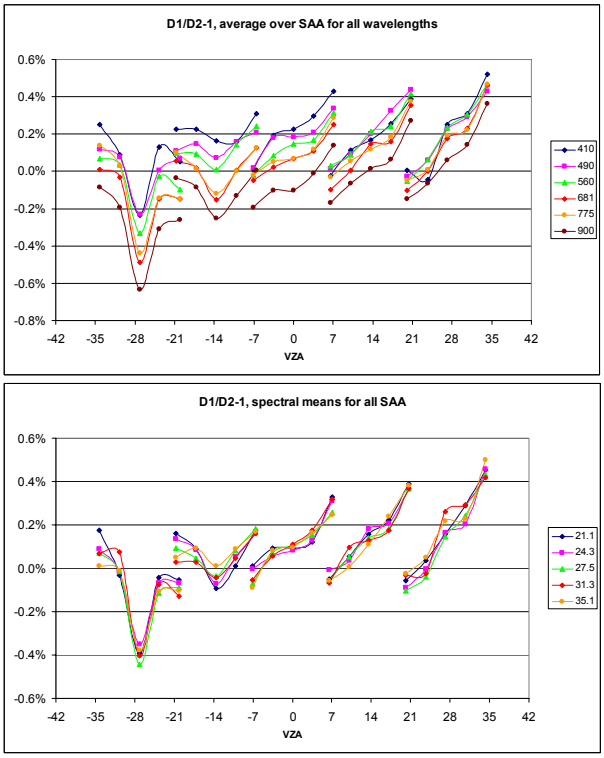


*Figure 6: Characterised diffuser BRDF relative difference.*

Characterisation has been performed in MERIS-like illumination and viewing conditions, including variations of the Sun azimuth angle due to seasonal effects. It has also been performed at several wavelengths, spread over the useful MERIS spectral range: 410, 490, 560, 681, 775 & 900 nm.

Characterisation showed almost identical BRDF for the two diffusers (see Fig. 6), allowing to define the diffuser ageing monitoring strategy described in the next section.

### 5.1.2 Diffuser BRDF model

The diffuser BRDF characterisation data has been used to derive an analytic model of BRDF as a function of observation geometry. A model depending only on Sun and View zenith angles and on relative azimuth angle has been selected as dedicated ground measurements showed that, to within the measurement accuracy, BRDF is insensitive to plate translation and rotation.

The selected model is the one of Rahman [5]. Its performances, reported on Fig. 7, are better than 0.3% RMS and ± 1% peak.

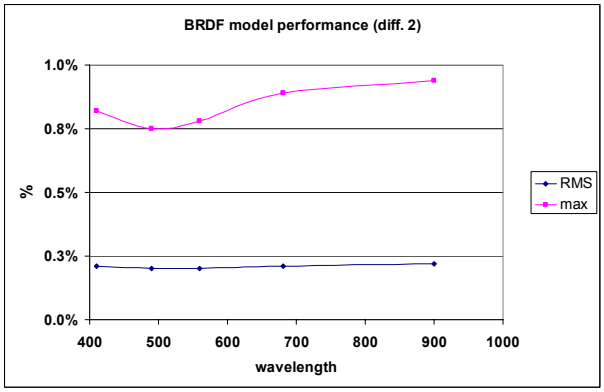


*Figure 7: performances of BRDF model for diffuser 2.*

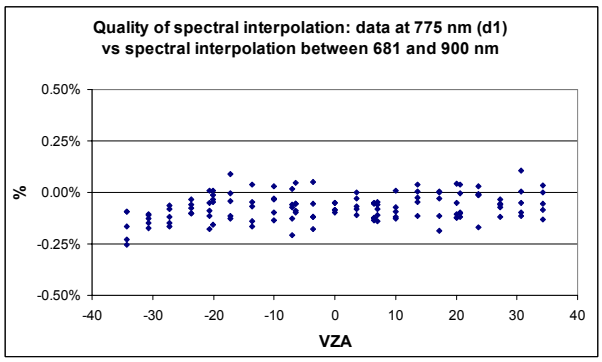


*Figure 8: performances of BRDF spectral interpolation*

The model is applied to characterisation data independently for each characterised wavelength.

Computation of the BRDF at a given wavelength is obtained by spectral interpolation. An example of spectral interpolation performance is shown on Fig. 7: BRDF at 775 nm interpolated between measurements at 681 and 900 nm (greatest wavelength step) have been compared to characterisation. The maximum error is les than 0.25%, RMS is around 0.1%.

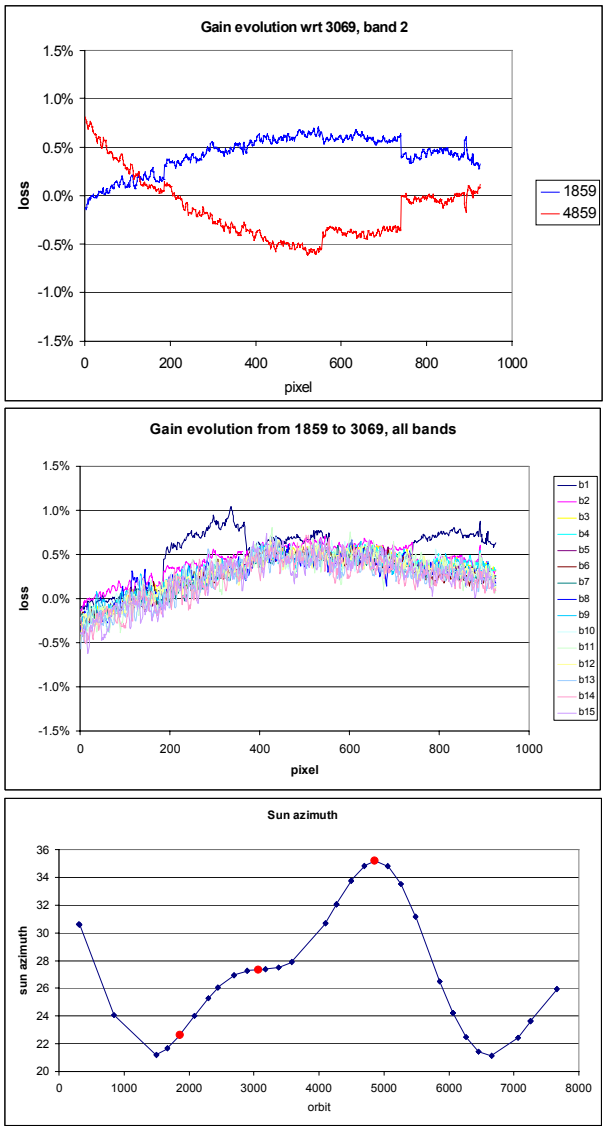


*Figure 9: Top: Relative Gain difference for band 2 (442 nm), orbits 1859 and 4959 relative to 3069, i.e. July 2002 and February 2003 relative to October 2002. Centre: same as top but extended to all bands and restricted to orbit 1859. Bottom: Corresponding Sun azimuth angles.*

Relative accuracy of the BRDF model applied on in-flight geometry conditions can be estimated through the analysis of Gain stability. Apart from the expected browning of the diffuser plate and optics, affecting mostly short wavelengths, instrument gain should stable with time and across field of view. Analysis of in-flight data show however a residual dependence of the computed instrument gains with Sun azimuth angle on the diffuser. The solar illumination azimuth angle varies throughout the year by more than 14 degrees. Fig. 9 show the relative evolution of gains obtained for two extreme azimuth angles with respect to a reference one obtained at a medium azimuth. It clearly shows that the curvature of the smoothly varying gain difference across the field of view changes sign with the azimuth difference. This change of curvature is directly correlated to the change of Sun azimuth, which leads us to believe that this effect is due to residual errors in the BRDF model. Centred peak error is ±0.5%.

It appears that, at least to first order, this residual error is independent of wavelength, as shown on Fig. 9-centre.

### 5.2 Diffuser ageing model

The diffuser plates have been exposed to a post-production processing in order to reduce the degradation (browning) of its scattering characteristics to space environment. According to on-ground simulations, the degradation over the mission lifetime should be minimal**.** However, as a means of verification, MERIS makes use of both its on-board diffusers to monitor the degradation of the frequently used (every 15 days) diffuser-1 by comparing it with the results from diffuser-2 which will be deployed only every 3 months. For these comparisons, the instrument is used as a transfer radiometer to compare measurements of diffuser-1 and diffuser-2 made for consecutive orbits, hence with almost identical illumination conditions. The comparison of the on-orbit calibration results using the two diffusers has confirmed that they have nearly identical BRDF - as expected from the on-ground characterisation [3].

By monitoring the, ratio of the two diffuser response, an estimate of the degradation of the frequently used diffuser-1 with respect to the reference diffuser-2 can be determined.

As of March 2006, Diffuser-1 has been exposed to approximately 170 min. of solar radiation, and shows a degradation at 412 nm of approximately 0.8%. According to the degradation study performed on-ground [4] a linear degradation can be expected for low illumination durations, which is confirmed by the degradation model – expressed in degradation per orbit - represented in Fig.10. As diffuser-2 has been exposed approximately 19 min., i.e. about 9 times less than diffuser-1, with the assumption that the degradation is due to exposure to solar illumination only, we can infer that diffuser-2 has suffered a degradation of less than 0.1% after the four years of the MERIS mission.

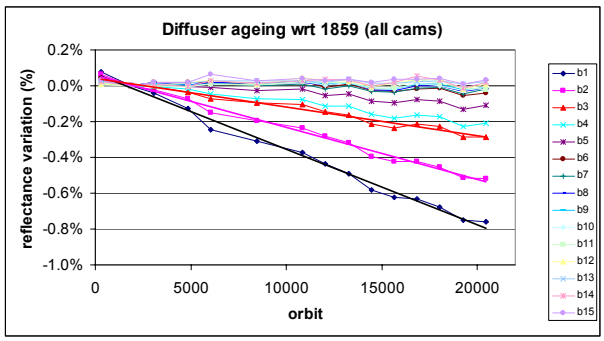


*Figure 10: relative evolution of diffuser response ratio.*

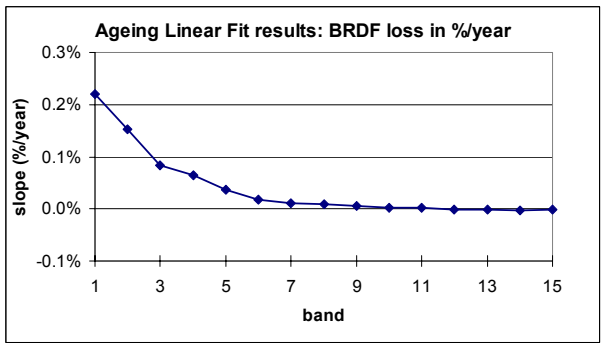


*Figure 11: diffuser ageing rate at MERIS channels wavelength, in percent per year.*

The diffuser ageing measurements have been linearly fitted and the results, expressed as reflectivity loss in percent per year is shown on Fig. 11 as a function of wavelength. The accuracy of the model is about 0.2% RMS. As it is highly correlated with the Sun azimuth variation, it is thought to be due mainly to the differences between the residual errors of the BRDF models for the two diffusers.

### 5.3 Instrument degradation model

The evolution of the instrument response for the period April 2002 to March 2006, based on diffuser 1 measurements corrected for diffuser ageing, has shown only a small degradation (Fig. 12) of the blue bands of less than 3%.

Optics is known to degrade exponentially in the space environment [6]. Barnes has developed a model for SeaWiFS which was also selected for MERIS. Starting from a reference value G($t_0$), the gain evolution with time follows

$$G(t) = G(t_0) \cdot (1 - \beta \cdot (1 - \gamma \cdot e^{-\delta t})) \quad (2)$$

where t is time, $t_0$ a time of reference, $\beta$ can be considered as the maximum degradation, $\delta$ as the time scale of the exponential and $\gamma$ as a time offset.

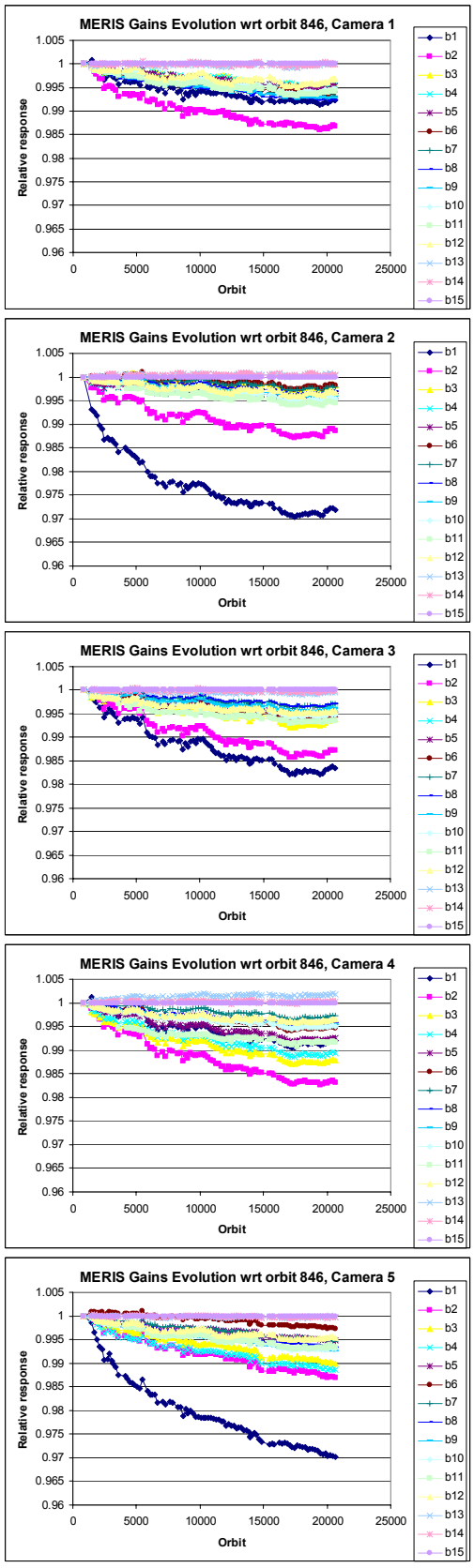


*Figure 12: mean per camera optics degradation for all bands. Cameras 1 to 5 from top to bottom.*

This parameterisation was applied on a per band and per pixel basis to MERIS for both resolutions (RR: 925 pixels, FR: 3700 pixels).

Due to the BRDF model limitations regarding dependency to Sun azimuth discussed in previous section, the evolution modelling has not been applied directly to gain measurements but to gains normalised to infra-red: as previously noticed, the model residual error is wavelength independent and optics degradation decreases with wavelength so that it should be negligible in the near-infrared. At the time this strategy was defined, direct verification of this latter assumption has been done using several orbits with very close azimuth angles, to get rid of most of the geometry residual error, allowing to estimate the instrument degradation (diffuser ageing is already known to be negligible in the IR) through simple gain ratios. The conclusion was that degradation in the IR is negligible, as shown on Fig.14-Bottom.

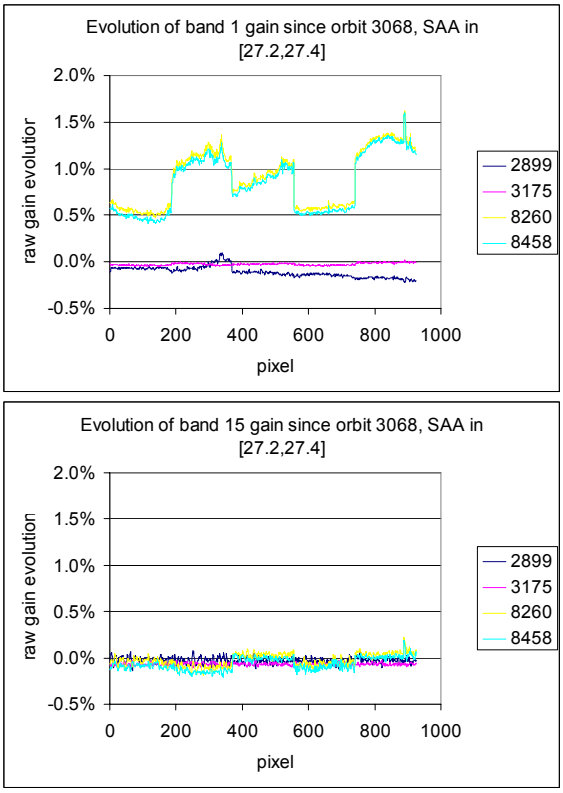


*Figure 14: Evolution of Instrument over 18 months for orbits with almost constant azimuth. Top: band 1 (412 nm) ; Bottom: band 15 (900 nm).*

Further monitoring of degradation using constant azimuth angle shows that this assumption has some limitations. Apparent degradation in the IR is now visible, varies greatly from camera to camera, and can reach 0.4% in camera 5 (Fig. 15). A study is foreseen to establish the impact on the model and define alternative strategy if required.

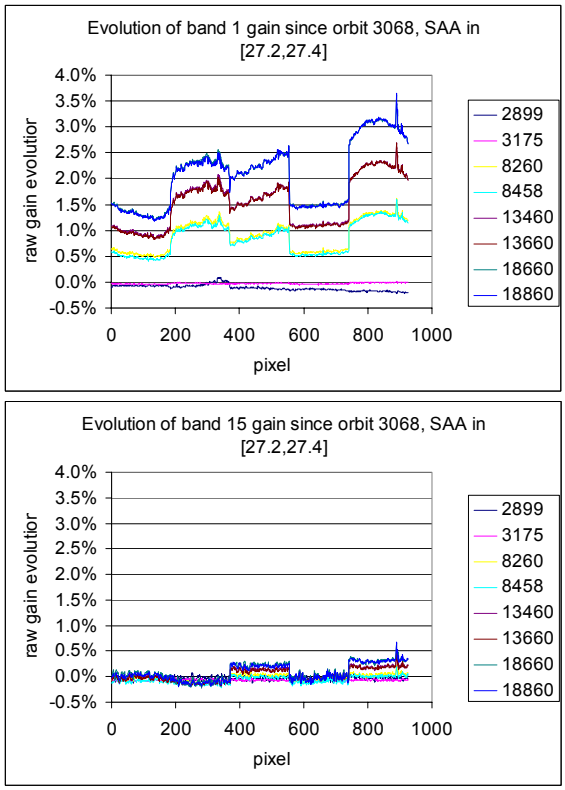


*Figure 15: Evolution of Instrument over 18 months for orbits with almost constant azimuth. Top: band 1 (412 nm) ; Bottom: band 15 (900 nm).*

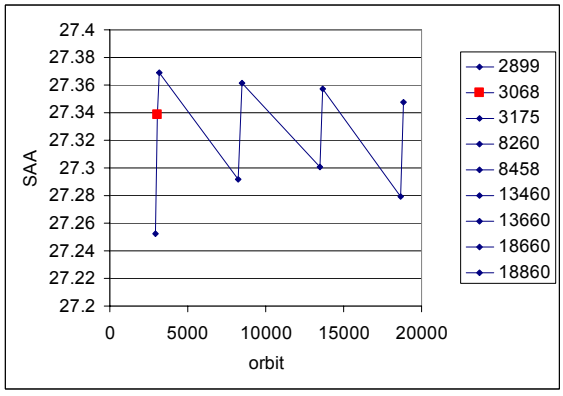


*Figure 16: Sun azimuth angle for the calibrations of Fig. 15.*

The model of Eq. 2 was thus computed in two steps. In the first step, time evolution was determined using normalisation to infrared, to remove geometry residual error, in addition to normalisation to a reference time. This reference time was selected as the calibration for which illumination condition was the closest to one of the diffuser plate BRDF on-ground characterisation. The second step consist in the determination of the reference gain by averaging a set of gain measurements

corrected for their time dependence using model of step 1.
This can be summarised as:

$$D_b(t,b) = \frac{G_b(t) \Big/ G_{15}(t)}{G_b(t_{ref}) \Big/ G_{15}(t_{ref})} = \Gamma_b \cdot (1 - \beta_b \cdot (1 - \gamma \cdot e^{-\delta_b t})) \quad (3)$$

$$\widetilde{G}_b(t_0) = \left\{ G_b(t) \cdot \frac{D_b(t_0)}{D_b(t)} \right\} \quad (4)$$

The combination of those two models can then be applied to calibration of Earth Observation measurements using:

$$G_b(t) = \widetilde{G}_b(t_0) \cdot D_b(t) \quad (5)$$

in Eq. (1).

An example of the relative gain evolution for band 1 of camera 5 is given on Fig.17-top. The result of the modelling is also displayed and shows good agreement with the measurement, as can be seen from the residual error of Fig.17-bottom (RMSE=0.0012).

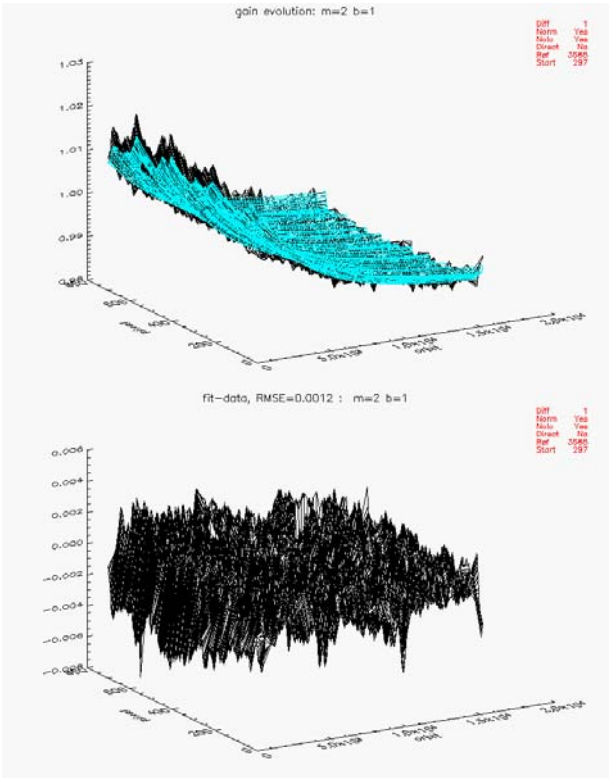


*Figure 17: Top: Evolution of Instrument response since orbit 846 for band 1 (412 nm) and camera 5 and corresponding degradation model. Bottom: Degradation model residual error*

The parameters of the model as expressed in Eq. 4 are shown for band 1 and all pixels on Fig. 18.

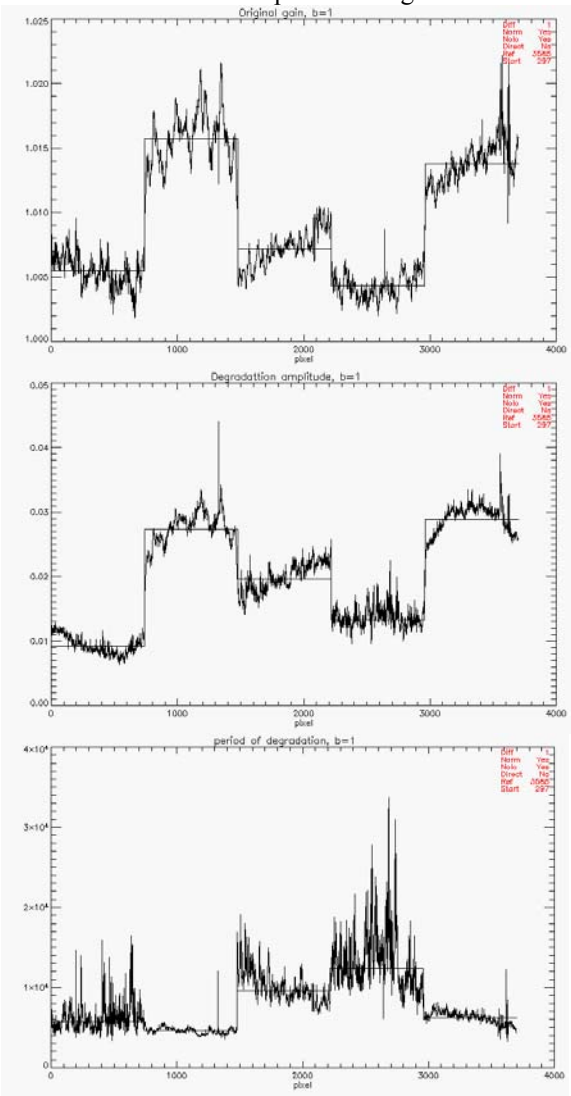


*Figure 18: Degradation model parameters for band 1, all cameras. From top to bottom: deviation from unity at ref. time, amplitude and time scale of the degradation ($\Gamma$, $\beta$ and $1/\delta$ of Eq. 3).*

This methodology has been applied to the calibration set available before starting the 2nd re-processing of MERIS RR data archive, i.e. up to orbit 15000, on diffuser 1 data only. The resulting model has been used for the whole re-processing, i.e. including in extrapolation for orbits up to about orbit 21000.

Quality of the modelling can be estimated through several estimators:

1. fit to data matching estimators on the fit data set
2. application to diffuser 2 (not used for model derivation) and fit to data match estimates
3. comparison with raw degradation estimates (using a set of calibrations at constant azimuth)

The fit to data match (modelling data set) is better than 0.1% RMS. Same estimator applied to diffuser 2, still restricted to the same time period, is even better. It is thought that this improvement is due to better quality of the BRDF model for plate 2. These results are shown on Fig. 19 (top: diffuser 1, bottom: diffuser 2).

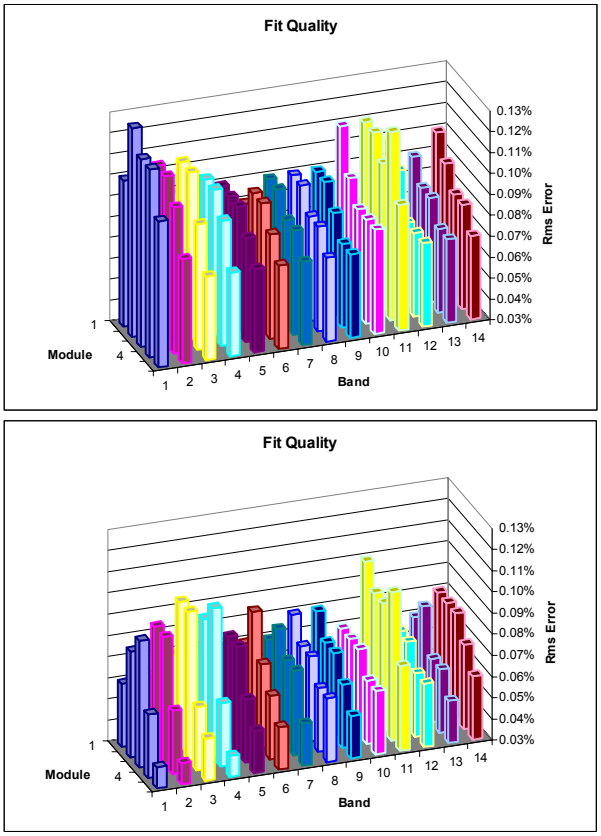


*Figure 19: model quality estimated through modelling RMSE. Top: diffuser 1 (model derivation data set), bottom: diffuser 2 data for the same time period.*

The set of orbits used to assess degradation in the infra-red can be used to compare model results with direct estimation of the degradation, providing that the diffuser plate ageing is accounted for. This set extends not only over the period used for model derivation but up to about one year later.
The results are shown on Fig. 20 for all pixels of band 1. Limitations of the model, in particular in extrapolation, appear immediately: it shows deviations of up to 0.6%.
It should be noted that deviation of degradation model from data shown on Fig. 20 looks very similar to the residual degradation of band 15 shown on Fig. 15.

These deviations are highly variable with camera and channel however. Fig. 21 show the per camera average of the model error for all bands (cameras 1 to 5 from top to bottom). The problem occur particularly for camera 3 (0.4%) and camera 5 (0.6%).

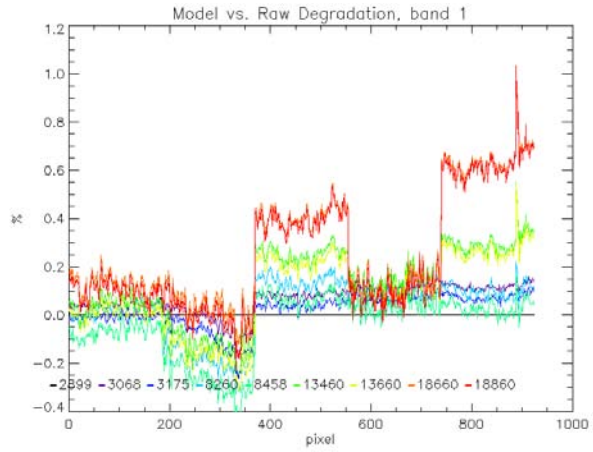


*Figure 20: Comparison of model to direct estimation of degradation using constant azimuth orbits, band 1, all pixels.*

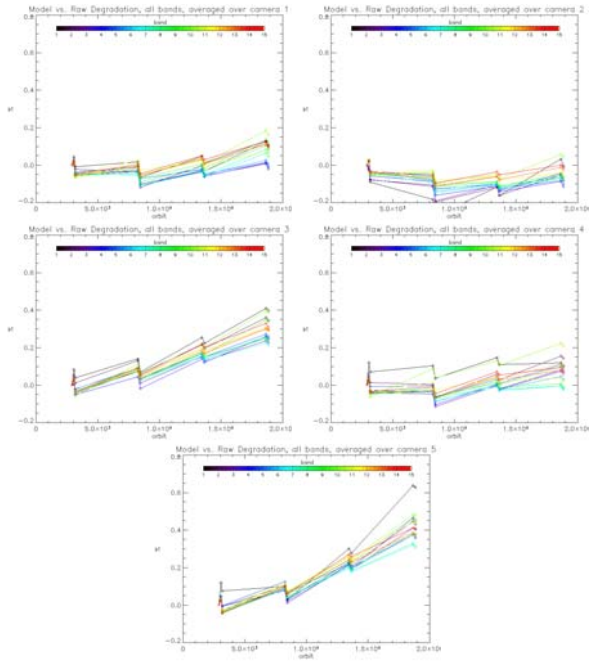

*Figure 21: Comparison of model to direct estimation of degradation using constant azimuth orbits, per camera averages as a function of orbit number, all bands. Cameras 1 to 5 from left to right & top to bottom.*

## 6 CONCLUSIONS

MERIS calibration relies on diffuser BRDF model and monitoring/modelling of diffuser ageing and instrument degradation.
BRDF models error budget (including ageing and geometry) is around 2%.
Current instrument degradation model error shows limitations, in particular when used in extrapolation.
Error for [2002,2005] is less than 1%, but rapidly increasing with time.
Total error budget is below 3%.

Degradation model and/or modelling methodology shall be improved in the near future to maintain current radiometric accuracy.
Error budget based on on-ground characterisation and in-flight data modelling shall be confirmed by indirect methods.

## 7 REFERENCES


Thuillier, G., M. Hersé, D. Labs, T. Foujols, W. Peetermans, D. Gillotay, P. C. Simon, H. Mandel, 2003, The solar spectral irradiance from 200 to 2400 nm as measured by the SOLSPEC spectrometer from the ATLAS and EURECA missions. *Sol. Phys*. **214** (1), 1–22.

Delwart S., Preusker R., Bourg L., Santer R., Ramon D. and Fischer J., MERIS in-flight spectral calibration, *Proceedings of the Second working meeting on MERIS and AATSR Calibration and Geophysical Validation (MAVT-2006)*.

Delwart S., Bourg L., Huot J.P.: MERIS 1st Year: Early Calibration Results. *Proc. SPIE* Vol. 5234, p. 379-390, 2004.

Chommeloux B., Baudin G., Gourmelon G., Bézy J-L., Van Eijk-Olij C., Groote Schaarsberg J., Werij H., Zoutman E.: Spectralon Diffusers used as in-flight optical calibration hardware. *Proc. SPIE* Vol. 3427, p.382-393, 1998

Rahman H., Pinty B., Verstraete M.M., Coupled surface-atmosphere reflectance (CSAR) model, 2, semi-empirical surface model usable with NOAA-AVHRR, Journal of Geophysical Research, Vol. 98, 1993.

Barnes R. A., Eplee R. E., Schmidt G. M., Patt F. S., and McClain C. R.: Calibration of SeaWiFS.I. Direct techniques," *Appl. Opt*. Vol. **40**, p. 6682-6700, 2001.